iScience

CellPress
OPEN ACCESS

Article

Electrosynthesis of dimeric butenolides by C-C-homocoupling in the oxidation of 2,4-diarylfurans under aqueous conditions

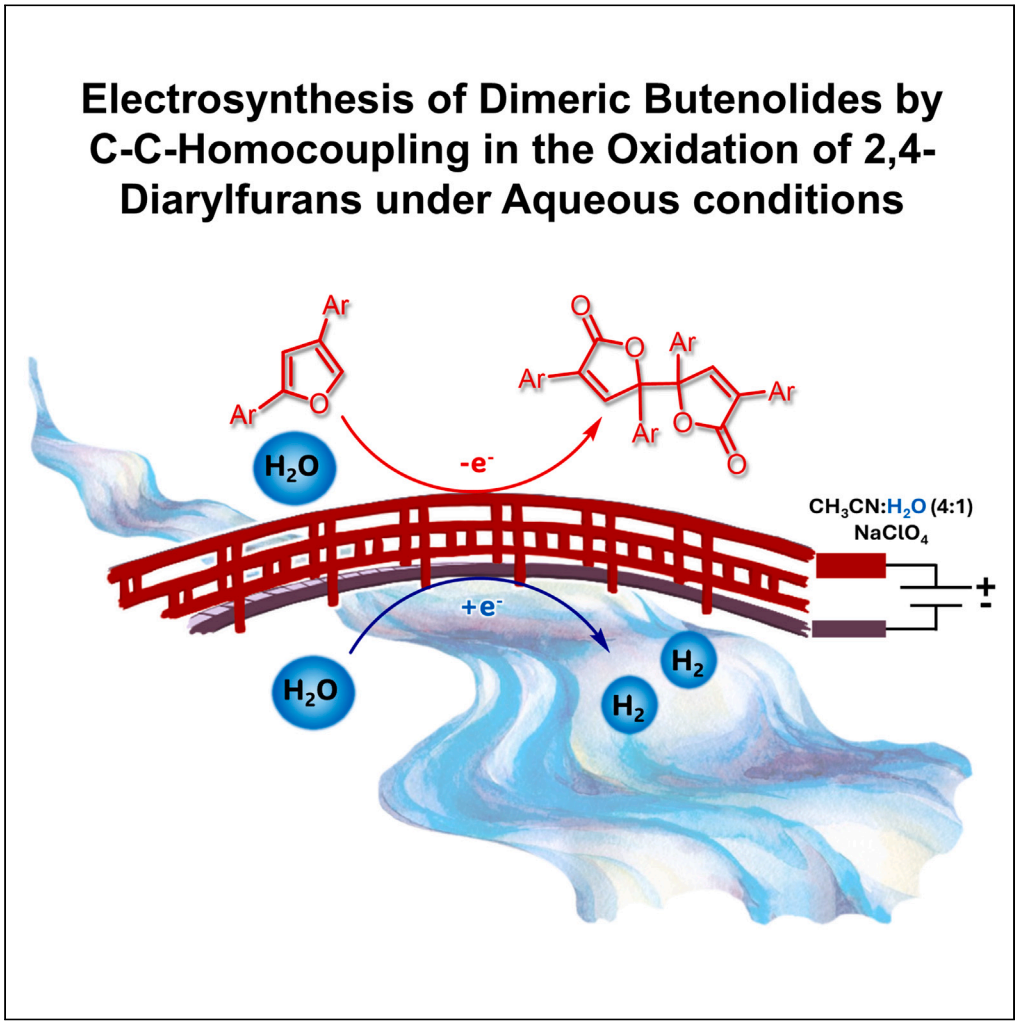

Belen Batanero, Noemi Salardon, Elena Prieto-Garcés, ..., Natalia Gómez-Casanova, Irene Heredero-Bermejo, José Luis Copa-Patiño

belen.batanero@uah.es

Highlights

Sustainable aqueous anodic oxidation of diarylfurans to bioactive butenolides

Clean and efficient galvanostatic synthesis of 5,5′-bis(3,5-diaryl-2(5*H*)-furanones)

Dimerization of furanoxyl radical intermediates through a C-C homocoupling reaction

DFT calculations to support the dimeric butenolides formation mechanistic proposal

Batanero et al., iScience *27*, 110765
September 20, 2024
https://doi.org/10.1016/j.isci.2024.110765

iScience

CellPress
OPEN ACCESS

Article

Electrosynthesis of dimeric butenolides by C-C-homocoupling in the oxidation of 2,4-diarylfurans under aqueous conditions

Belen Batanero,[1,3,*] Noemi Salardon,[1] Elena Prieto-Garcés,[1] Lorena Herrera,[1] Soufyane Er-Ryhy,[1] M. Teresa Quirós,[1] Natalia Gómez-Casanova,[2] Irene Heredero-Bermejo,[2] and José Luis Copa-Patiño[2]

SUMMARY

Fast and efficient galvanostatic conversion of 2,4-diarylfurans into dimeric furan-2(5*H*)-ones is now possible in one pot and good yields at room temperature in sustainable aqueous organic solvent. Recent applications of these highly desired structures demand our attention since they are a versatile alternative to acrylates in polymerization to achieve green materials. The reaction mechanism proposal, supported by density functional theory (DFT) theoretical calculations, involves furanoxy radicals, detected by electron paramagnetic resonance (EPR), as the last intermediate before a homocoupling step that affords butenolides. The process can be successfully extended to an array of electron-donating and electron-withdrawing substituents on the aromatic ring. The proposed pathways to explain the formation of the products are rationalized and discussed. A concomitant oxidation of water to hydroxyl radicals is not discarded, particularly with electron-withdrawing substituents at the aromatic ring. In addition, the biological activity as biocides of the obtained compounds was tested, and they showed promising activity against *Staphylococcus aureus*.

INTRODUCTION

Furan-2(5*H*)-ones (α,β-butenolide core moieties) are important building blocks in organic chemistry that are present in many natural products and show potent bioactivity. These molecules have been evaluated for their use as anti-inflammatories,[1] in cancer therapeutics[2] or as antifungal agents[3,4] among others. Particularly, 5-aryl-γ-lactones are considered a kind of "chemical defense" as they have been collected from microorganisms grown in harsh environments.[5]

However, recent consideration is being focused[6] on increasing the applications of furan-2(5*H*)-ones (α,β-unsaturated five-membered cyclic esters). These structures are finding uses as potential monomers (by structural similarity with acrylates) to access green materials[7,8] able to replace the oil-derived polymers used in plastics, adhesives, resins, or paints. A subclass of 5-acyloxybutenolides has just been described[9] to enhance the reactivity of 5-alkoxy and unsubstituted butenolides toward radical copolymerization, making them a versatile bio-based alternative for acrylates in coating compositions. Besides, γ-butenolides are important synthetic precursors of γ-butyrolactones by conjugate reduction processes.[10] The latter being highly useful and versatile starting materials to synthesize physiological and therapeutical target molecules such as pilocarpine or arctigenin.[11]

Although the butenolide scaffold is ubiquitous in nature, the development of new chemical transformations that simplify the synthesis of valuable building blocks is a challenging task in organic chemistry. For that reason, synthetic approaches to butenolides have been reviewed,[12] many of them involving enantioselective methodologies for the total synthesis of pharmaceutically active molecules. The synthesis of γ-methylenebutenolides has just been accomplished through an indium-promoted lactonization of (indol-3-yl)-2-oxoacetaldehydes,[13] or by palladium-catalyzed cyclocarbonylation of aryl halides with acetylenes.[14] β-Arylbutenolides, which are synthetic intermediates for obtaining complex compounds such as rubrolides,[15] are prepared using tetronic acids in a reaction mediated by $BF_3.OMe_2$[16] or via a regioselective Pd-catalyzed reaction with aryl(trialkyl)stannanes.[17] The α,γ-diphenylbutenolide was obtained in 1965 by Volger et al.[18] after oxidation of *dypnone* (1,3-diphenyl-2-buten-1-one) by oxygen in a reaction catalyzed by cupric-amine complexes in an alkaline methanolic solution. Later, the α,γ-diphenylbutenolide structure was photochemically transformed into the bis-lactone 4,4′-bis(2,4-diphenylbut-2-en-4-olide) by Gopidas et al.[19] in low yield and through a mechanism involving fluorescent furanoxy radicals.[20]

The use of furans as starting molecules to get monomeric butenolides was achieved by the photo-oxygenation of α-unsubstituted furans by singlet oxygen providing 5-hydroxy-furan-2(5*H*)-ones[21] (Figure 1) and involving a furan endoperoxide intermediate. This reaction was faster

[1]University of Alcala, Department of Organic Chemistry and Inorganic Chemistry and Institute of Chemical Research Andrés M. del Rio, 28805 Alcala de Henares, Madrid, Spain
[2]University of Alcala, Department of Biomedicine and Biotechnology, 28805 Alcalá de Henares, Spain
[3]Lead contact
*Correspondence: belen.batanero@uah.es
https://doi.org/10.1016/j.isci.2024.110765

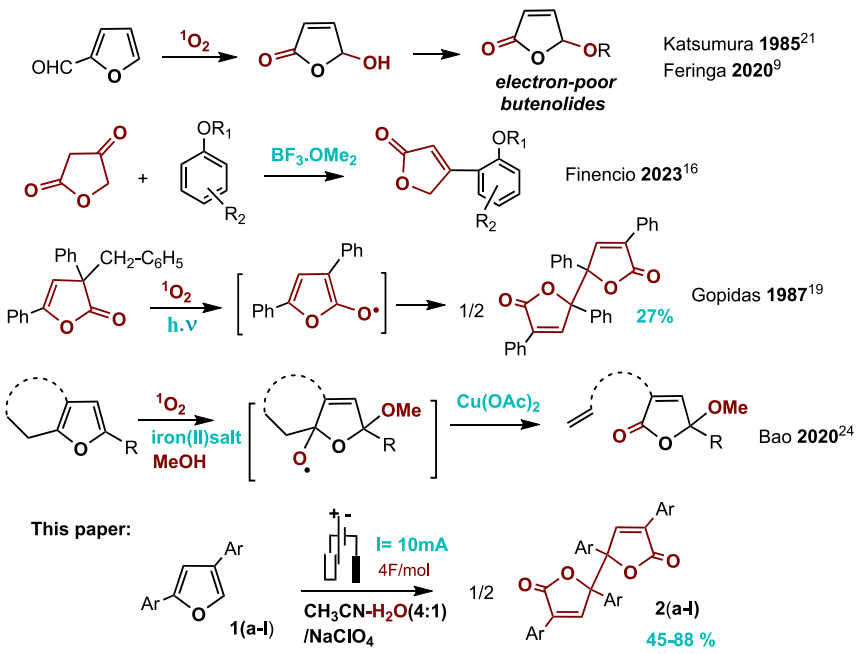

Figure 1. Butenolides prepared from furan ring as starting material

in the presence of a sensitizer.[22,23] More recently, iron(II)-mediated radical fragmentation of furans in the presence of $Cu(OAc)_2$ has been reported.[24] Furthermore, H_2O_2 oxidation of furfural, obtained in large scale from biomass, afforded 2(5*H*)-furanone[25] in 71% yield after 24 h of vigorous stirring in aqueous acetic acid. In addition, Torii et al. described the anodic oxidation of 5-alkyl-2-furoic acids in acetic acid-methanol, to afford 5-alkyl-5-methoxy-butenolides as the major products after initial formation of the corresponding 2,5-dimethoxy-dihydrofuran intermediates.[26]

Some of the many advantages that electrochemistry provides as a sustainable[27] tool in organic synthesis is the possibility of synthesizing organic frameworks through C−C bond formation, via the activation of the substrate by electron transfer at normal pressures and temperatures, avoiding the need for the classic thermal activation. Anodic C-C homocoupling reactions have been achieved in a one-pot procedure since Weinberg pioneering description of aromatic dehydrodimerization,[28,29] Kolbe dimerization-decarboxylation,[30–32] or Dryhurst dimerization of nitrogenated heterocycles[33] at the anode. Many recent synthetic applications of such processes are still being published, such as the electrolysis of medium chain carboxylic acids to get fuels at technical scale[34] or the efficient electrosynthesis and doping of polycyclic aromatic hydrocarbon semiconductor films.[35]

Furans have never been oxidized at the electrode with the aim of transforming them into bis-butenolides through C–C bond formation (homocoupling). Now, this oxidation reaction is described in a single-step electrochemical process, and further insights to the mechanism proposal are given. In addition, the *in vitro* antibacterial activity of these products against *Staphylococcus aureus* has been confirmed. The practical utility of our transformation could be applied to other π-excedent oxygenated heterocyclic substrates, such as the oxazole ring which, through this homocoupling reaction, could quickly and sustainably be converted into products with high added value.

RESULTS AND DISCUSSION

Anodic preparation of butenolides

Dimeric 3,5-diarylfuran-2(5*H*)-ones **2(a-l)** have been easily prepared in one-pot and good yield from their parent 2,4-diarylfurans **1(a-l)** via anodic oxidation in acetonitrile/water or dimethylformamide (DMF)/water mixtures and $NaClO_4$ as solvent-supporting electrolyte system (SSE) under both, constant current (galvanostatic) or constant potential (potentiostatic) conditions. The nature of SSE clearly determined the structure and distribution of obtained products, being the amount of water of decisive importance to avoid the formation of oligomers[36] (Scheme S1) at the expense of butenolides **2**. However, an excess of water could also result in undesired overoxidation products. Figure 2 shows the cyclic voltammetry of **1a** in dry acetonitrile and the effect on it of water addition (10%) to the SSE solution.

Anodic oxidation of electron rich five membered heterocycles, pyrrole[37] or thiophene[38] has been largely studied to get, after being deposited, conducting polymers or polythiophenes with interesting optoelectronic properties, respectively. However, polyfurans have scarcely been explored[39] due to their difficult polymerization and low stability after exposure to oxygen and light. Nevertheless, the electrochemical oxidation of alternating benzene-furan triarylated oligomers[40] was studied under aprotic conditions.

In this context, our research group described in 2021 the anodic oligomerization of 2,4-diphenyfuran (**1a**)[36] when oxidized using dry acetonitrile-$LiClO_4$ as SSE. The behavior of **1a** was similar to that already observed in other five membered heterocycles.

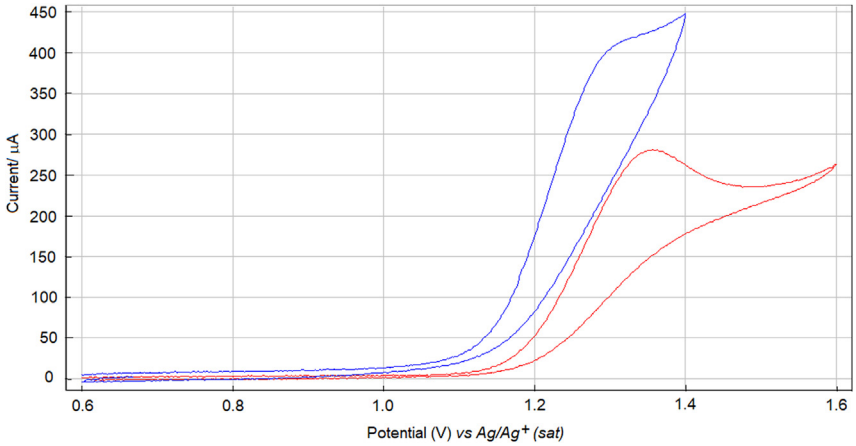

Figure 2. Cyclic voltammetry of 2,4-diphenylfuran (1a) in dry acetonitrile (red curve) or in acetonitrile-H_2O (10:1) mixture (blue curve)/$LiClO_4$ (0.1 M) as SSE, at Pt/Pt as working and auxiliary electrodes and Ag/Ag^+ (sat) as reference electrode

Scan rate: 100 mV/s.

Now, when this electrolysis is conducted in the presence of a 20% of water, the reaction evolves to dimeric butenolides **2** in a good yield. These products have a fairly low solubility in the electrolysis medium which, in many cases, permits their easy isolation by filtration as the only elaboration process, allowing, at the same time, their separation from the reaction side products.

The experimental conditions of this anodic conversion were optimized using **1a** as model substrate and modifying the type of reactor (with/without separation of electrolytic compartments), the solvent (acetonitrile or DMF), the water content, the electrolyte, the temperature, the anode material, and the use of a constant current (10, 30, and 50 mA) or a constant potential (+1.3 V vs. Ag/Ag^+) conditions. The results are summarized in Table 1.

When preparative-scale oxidation was performed in the absence of water or with only a 5% of water in the SSE (entries 1 and 2 in Table 1), the oligomerization was the main process, as expected considering that water is the source of oxygen in the dimeric butenolide. A water content of 20% (ACN/H_2O (40:10), entry 3), close to the maximum allowed before **1a** precipitates, was favorable to get a 73% yield of dimeric butenolide **2a** (Scheme 1, route 1). The use of undivided cell (entry 4) produced an important decay on the yield of **2a**, probably due to intermediate species diffusion to the cathode, where they are reduced to undesirable products consuming some starting material. An increase of the current density to 30 or 50 mA (entry 5) afforded a lower yield of **2a** (60 or 53%, respectively). This result is consistent with a larger anodic discharge of water to hydroxyl radicals which, after 1,4-addition across the diene system of the starting furan, may lead to the anodic formation of 5-hydroxy-3,5-diphenyl-2(5*H*)-furanone (**3a**) as a secondary product (see Scheme 1, route 2).

A constant potential experiment was performed (entry 6) setting a value of +1300 mV (vs. Ag/Ag^+). The electrolysis led to a slight decrease in the yield of **2a**, probably due to an increase in the competitive oxidation of water (Figure 2). The use of DMF instead of CH_3CN was a good option with some of the insoluble starting furans. When DMF was used in the oxidation of **1a** (entry 7), a good yield was also registered. However, the use of a mixture CH_3CN-MeOH (30:20) (entry 8) gave no trace of the dimeric butenolide. In this case, (*Z*)-methyl 4-oxo-2,4-diphenylbut-2-enoate was isolated as the main product, which formation might arise from the hydrolysis of 5-methoxybutenolide (Scheme 2). A lower temperature (entry 9) hindered the complete dissolution of the initial furan and therefore decreased the concentration of proposed furanoxy radicals (**ii**) that should dimerize to lactone **2** on the anode surface (see Scheme 1). The influence of the anode material was studied (entry 10) by applying the experimental conditions of entry 3 (Table 1) in graphite. As it is well known, carbon centered radicals are easily converted to carbocation intermediates at a graphite anode.[41,42] This fact minimizes any possible homocoupling to dimeric butenolide, while favoring a nucleophilic attack by water or by another furan molecule. In this case, the bis-lactone **2a** was not obtained, and the electrolysis conducted to 3,5-diphenyl-5-(3,5-diphenylfuran-2-yl)-furan-2(5*H*)-one (**4a**) (Scheme 1) after the furanoxy radical (**ii**) was subsequently oxidized to a carbocation that was finally attacked by another molecule of **1a**.

The electrolyte effect in the formation of **2** was also analyzed. The use of Et_4NBr (entry 11), yielded 2-bromo-3,5-diphenylfuran as the only product, obtained through a first oxidation of bromide to Br_2 that afterward is added to the heterocycle. Halide-free electrolyte Bu_4NBF_4 was tested in entry 12, affording **2a** in 50% yield and being 3,5-diarylfuran-2(5*H*)-one and 5-hydroxyfuranone **3a** the side products. In this case, the former compound is suggested to be mainly formed after a hydrogen atom abstraction (from the electrolyte butyl chain) by the furanoxy radical intermediate (**ii**).

The electrolysis was definitively optimized by increasing the concentration of **1a**, working with twice the equivalents of furan and half the volume of the previous experiments. Successfully, compound **2a** was obtained in 80% yield (entry 13), as expected when a dimerization (homocoupling) of carbon centered radicals is involved (Scheme 1).

Starting with the almost optimized experimental conditions, the scope of this oxidative dimerization reaction was investigated by incorporating different substituents in the benzene ring of the starting 2,4-diarylfurans **1(a-l)** (Table 2). Several functionalities, including both electron-donating and electron-withdrawing groups, were well-accommodated and delivered the corresponding dimeric butenolides **2(a-l)**.

Table 1. Oxidation of 1a (0.25 mmol) at Pt anode

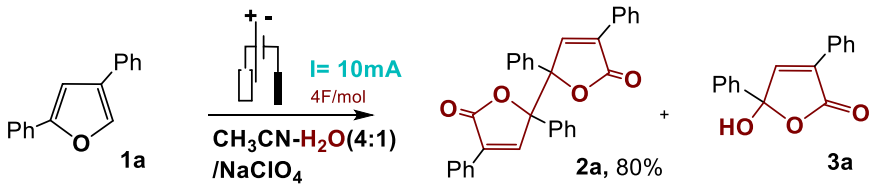

Entry	*Solvent* (mL)	*Electrolyte* (0.1 M)	I (mA)	Yield of 2a (%)	Observations
1	ACN (40)	$LiClO_4$	10	not obtained	only oligomerization
2	ACN/H_2O (40:2)	$NaClO_4$	10	20	80% oligomers
3	ACN/H_2O (40:10)	$NaClO_4$	10	73	
4	ACN/H_2O (40:10)[a]	$NaClO_4$	10	45	Intermed cathodic reduction
5	ACN/H_2O (40:10)	$NaClO_4$	50[b]	53	side product **3a**
6	ACN/H_2O (40:10)	$NaClO_4$	+1.3 V[c]	63	
7	DMF/H_2O (40:10)	$NaClO_4$	10	70	
8	ACN/MeOH (30:20)	$NaClO_4$	10	not obtained	keto-methylacrylate
9	ACN/H_2O (40:10)	$NaClO_4$	10[d]	60	side product **3a**
10	ACN/H_2O (40:10)	$NaClO_4$	10[e]	5	Compound **4a** as main product
11	ACN/H_2O (40:10)	Et_4NBr	10	not obtained	2-bromofuran main product
12	ACN/H_2O (40:10)	Bu_4NBF_4	10	50	side diarylfuran-2(5*H*)-one
13	ACN/H_2O (20:5) [f]	$NaClO_4$	10	80	

Temp 25°C. 4.0 F/mol. Obtained results after modifying different reaction parameters to optimize the formation of dimeric butenolide **2a**.
[a]Undivided cell.
[b]When I = 30 mA a 60% yield of **2a** was obtained.
[c]Ag/Ag^+(*sat*) as the reference electrode.
[d]T^a = 15°C.
[e]Graphite anode.
[f]Oxidation of 0.5 mmol **1a** in ACN/H_2O (20:5) (concentration of **1a** four times higher than in entry 3).

4-Alkylphenyl groups such as **1b** (45%) and **1c** (20%), as well as other electron-donating substituents (EDG) (4-dimethylaminophenyl group not included in Table 2), afforded lower yields on **2**, due to the formation of side-chain oxidation products instead of the dimeric butenolides. Nevertheless, steric effects and low solubility of some furans are probably also involved in the final homocoupling reaction that is hindered when bulky substituents in 2-position, such as 2-naphthylfuran (**1f**), are electrolyzed. Surprisingly, diarylfurans with strong electron-withdrawing substituents (EWG) in 4-position of the phenyl ring, such as cyanide (**1l**), gave only a 20% yield of **2l** when the optimized experimental conditions of entry 13 (Table 1) were applied. In this case, the starting material was partially recovered after electrolysis. These results can be rationalized to some extent because these systems (**1h** or **1l**) exhibit a more positive oxidation potential than **1a** (see Figure S1), and when a constant current of 10 mA was applied, the water discharge seemed the main competitive electrochemical process. However, an increase of the current to 30 mA improved the yield of **2l** from 20 to 65%, with only a 30% of recovered starting furan **1l**.

To better understand and gain further insights into the mechanism of this transformation, some control experiments were conducted with **1a** (see Scheme 3).

The coupling products of the furanoxy radical (**ii**) with BHT (2,6-di-tert-butyl-4-hydroxytoluene) and with BQ (1,4-benzoquinone) were detected by GC-MS (gas chromatography coupled to mass spectrometry) (see GC-MS data in supporting information). This fact supports the suggested formation of **ii** as a reaction intermediate. Furthermore, the detection by GC-MS of 3,5-di-tert-butyl-4-hydroxybenzaldehyde, derived from the coupling of BHT with hydroxyl radical[43] bears out a simultaneous oxidation of water to hydroxyl radicals, as expected with furans **1(g-l)** due to their more positive oxidation potentials. The cyclic voltammetry of **1g** (see Figure S1) shows that, when water is added to a dry SSE solution containing **1**, the oxidation peak potential clearly advances to a less positive value, increasing at the same time its peak current. These results are in agreement with some published works[30,44–46] that did not discard the formation of hydroxyl radicals under similar aqueous anodic conditions.

According to these results, a mechanistic proposal that would explain the formation of bis-lactone (**2**) formation at the anode is shown in Scheme 1. Initial direct discharge of **1** evolves to a benzylic radical intermediate (**i**) after a water molecule nucleophilic attack. Further oxidation of **i** (route 1) would lead, after loss of a proton, to 3,5-diaryl-2-hydroxyfuran molecules (this were in some cases isolated as minor products in their tautomeric 3,5-diarylfuran-2(5*H*)-one form). Additional anodic discharge of this furanone (activated hydroxy furan) would evolve to the corresponding furanoxy radical (**ii**) detected by electron paramagnetic resonance (EPR) (Figure S2) when **1g** was oxidized. A final C-C

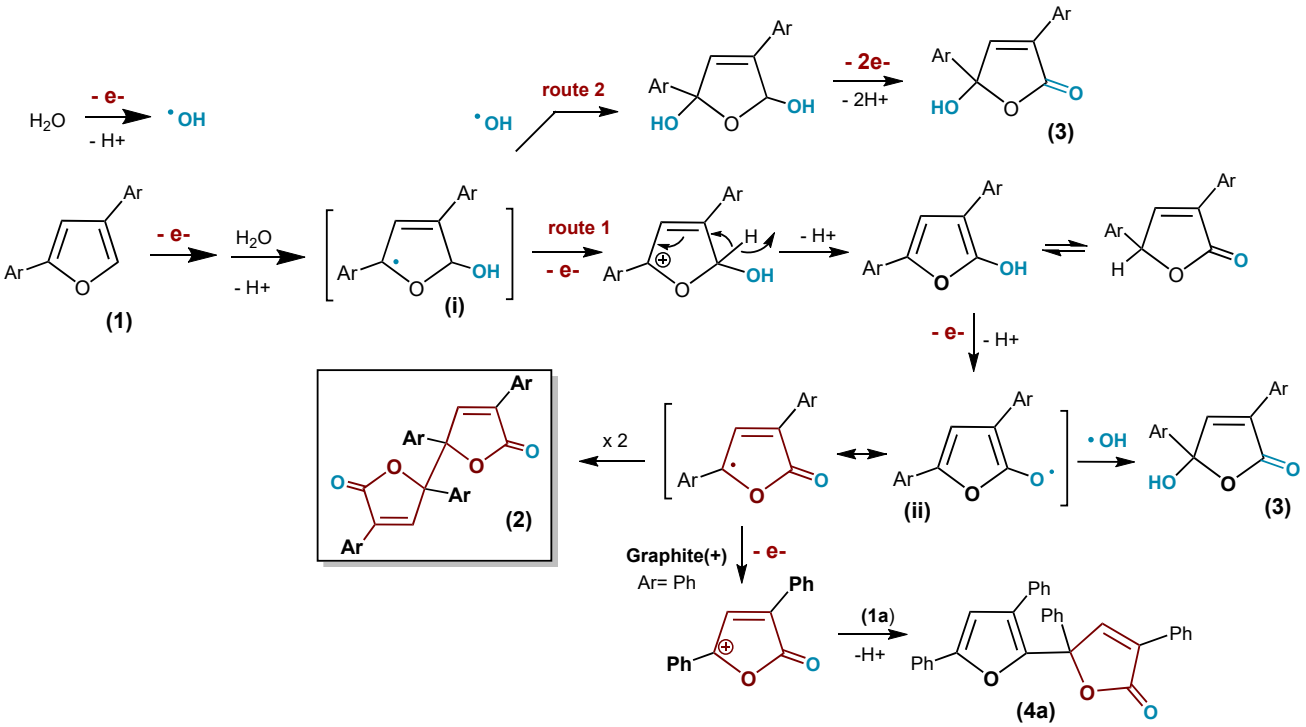

Scheme 1. Suggested mechanistic pathway to explain the formation in ACN/H_2O of dimeric butenolides 2 and other side products

homocoupling reaction involving two furanoxy radicals would provide **2** in a process that involves a global coulombimetric charge consumption corresponding to 3 F per molecule of starting furan.

Simultaneously, an excess of hydroxyl radical in the medium could transform intermediate **i** into a 2,5-dihydroxy-2,5-dihydrofuran (route 2) which, after being further oxidized, would evolve to the isolated secondary product **3**. However, this is not the main reaction pathway, as should be (according to the computational studies shown in the following text) if the formation of hydroxyl radicals was the main oxidation event.

When electrolysis is performed in acetonitrile:methanol (30:20) (Table 1, entry 8), the presence of CH_3OH (instead of water) further advances the anodic peak potential in the cyclic voltammetry of **1a**. Methanol is more easily oxidized[47] than water and, under constant current (10 mA) conditions, the formation of methoxyl radicals becomes a plausible process. In this reaction no traces of the dimeric butenolide **2a** were registered, instead, the corresponding (*Z*)-methyl 4-oxo-2,4-diphenylbut-2-enoate was obtained (Scheme 2).

The mechanism proposal to get dimeric butenolides **2** was analyzed by computational methods in order to support the pathways presented in Scheme 1.

Theoretical calculations

A computational study with DFT calculations was performed in gas phase at B3LYP/6-311G(d,p)(C,H,O)//B3LYP/6-31G(d)(C,H,O) level and using **1a** as the model substrate. To take into account the influence of the potential in the reaction energies of each elementary step, the

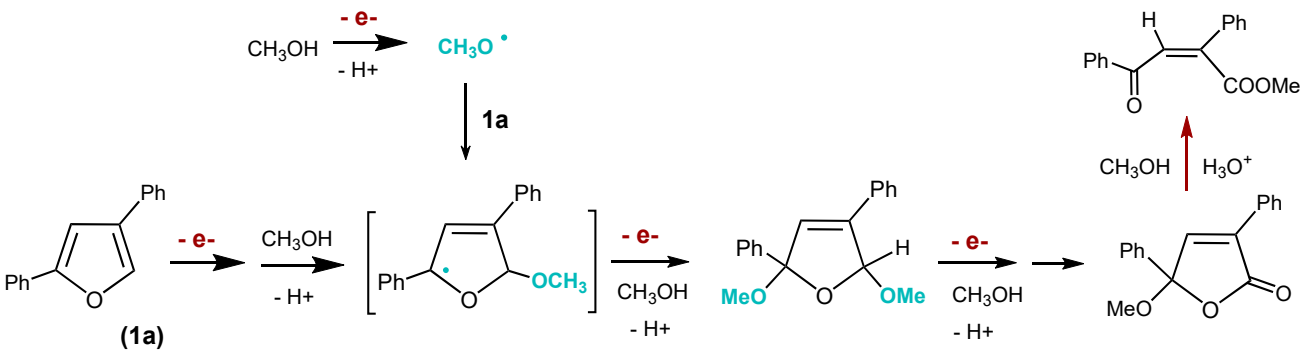

Scheme 2. Mechanism proposal in the anodic oxidation of 1a in ACN/MeOH (30:20) mixture as the solvent

Table 2. Obtained results in the oxidation of 1(a-l) in ACN/H_2O or DMF/H_2O-$NaClO_4$ as SSE in a divided cell under galvanostatic I = 10 mA conditions at room temperature and Pt/Pt as electrodes

Ar	*SSE* (0.1 M $NaClO_4$)	Yield of 2 (%)
a: Ph	ACN/H_2O (40:10)	73
b: 4-Me-C_6H_4	ACN/H_2O (40:13)	45
c: 4-Pr-C_6H_4	ACN/H_2O (35:10)	20
d: 4-MeO-C_6H_4	ACN/H_2O (40:10)	47
e: 4-EtO-C_6H_4	DMF/H_2O (35:8)	52
f: 2-Naphthyl	DMF/H_2O (55:9)	44
g: 4-Cl-C_6H_4	ACN/H_2O (36:12)	82
h: 2,4-diCl-C_6H_4	ACN/H_2O (40:8)	51
i: 4-Br-C_6H_4	ACN/H_2O (35:10)	72
j: 4-F-C_6H_4	DMF/H_2O (45:10)	60
k: 4-$MeSO_2$-C_6H_4	DMF/H_2O (45:11)	88
l: 4-CN-C_6H_4	DMF/H_2O (40:10)	20 (65)[a]

[a]I = 30 mA.

computational hydrogen electrode (CHE) model was used,[48] considering a potential of +1.3V. In the steps entailing oxidation processes, only the thermochemistry has been considered by computing elementary reaction free energies. The computed energy profile for the different reaction pathways is depicted in Figure 3. The overall profile of route 1 goes downhill, being energetically favored. Only the last homocoupling step is slightly endoergonic (0.17 to 0.23 eV for the formation of the meso dimeric butenolide and the enantiomeric mixture, respectively), which accounts for the exceptional stability of furanoxi radicals. The spin density map of intermediate (ii) (see Figure S3), shows that the unpaired electron is mainly centered in carbons 3 and 5 (16.5% and 17.1% of contribution to the spin density, respectively), with the contribution of oxygen being lower (10.4%).

The energy profile for route 2 has also been computed. The overall decrease in energy for the formation of product **3** is higher than the stabilization obtained with the formation of dimeric butanolide **2** (5.54 vs. 3.25 eV). This result suggests that, if the formation of hydroxyl radicals was the main oxidation event in the media, product **3** would be the major product obtained. The reaction energy for the formation of hydroxyl radicals from water is 1.18 eV, which indicates that, although the oxidation of water is possible under the reaction conditions, the energy required for it to occur is quite high, and thus it would not be the main process (see Figures S4 and S5).

On the other hand, the reaction energy for the formation of methoxy radicals from methanol is 0.48 eV. The oxidation of methanol is energetically more favorable than the oxidation of water, which explains why, when methanol is used instead of water, only the product that would arise from route 2 is obtained.

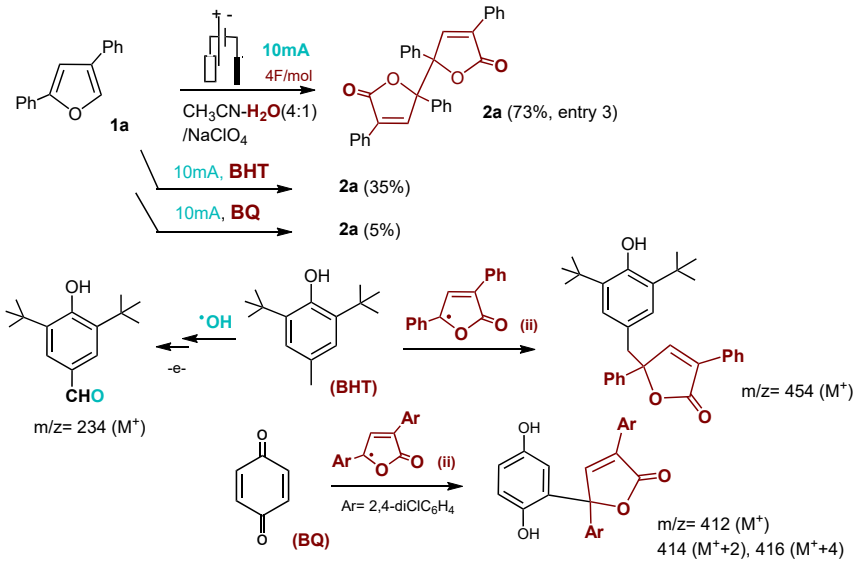

Scheme 3. Control experiments that support a radical mechanism in the formation of 2

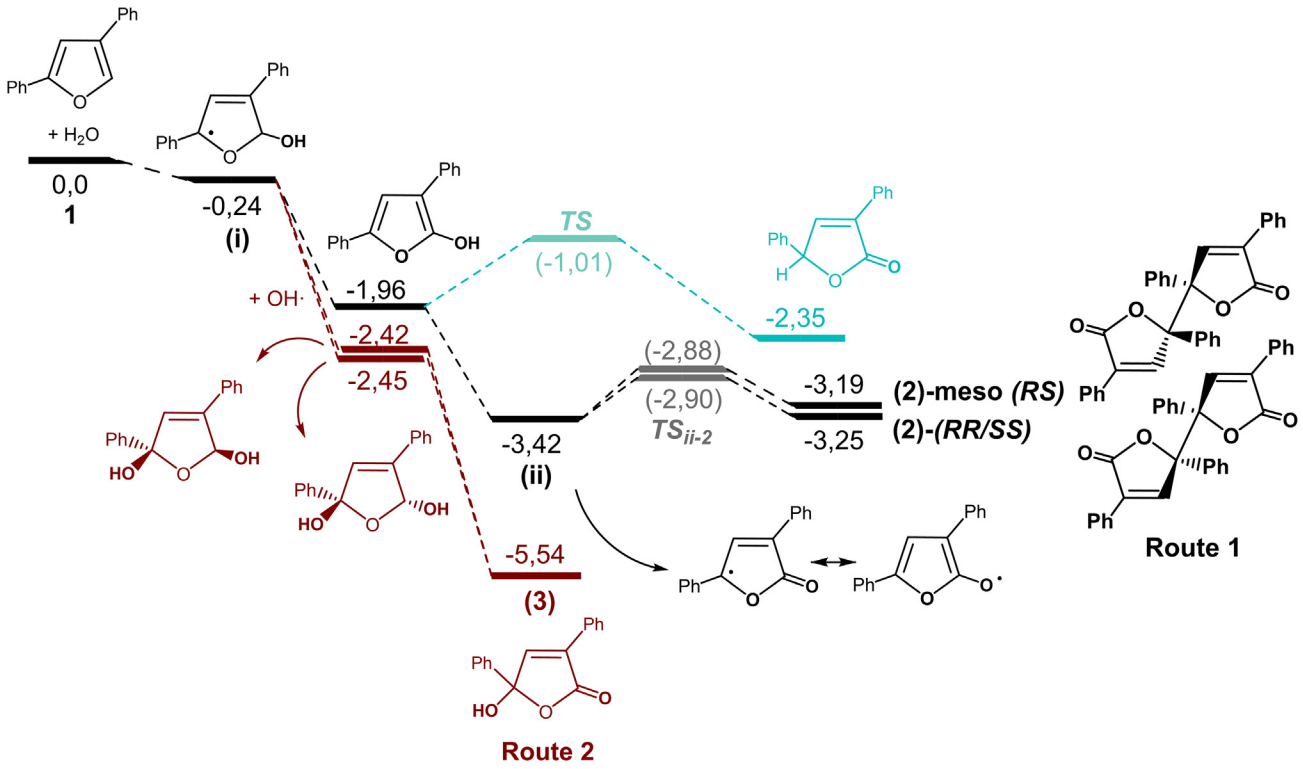

Figure 3. Calculated reaction profile for the oxidation of 2,4-diphenylfuran 1a (B3LYP/6-311G(d,p)(C,H,O)//B3LYP/6-31G(d)(C,H,O))

ΔG in eV and activation energies in brackets.

The aforementioned experimental evidence, in addition to these DFT calculations and the characterization of the different reaction by-products, validates the mechanism proposal presented in Scheme 1, which seems the most reasonable to explain the anodic formation of dimeric butenolides **2** when performed in aqueous-organic solvents.

Antibacterial activity

To show the biological applicability of the obtained butenolides, their antibacterial activity against *Staphylococcus aureus* was assayed. Studies showed that 5,5′–bis(3,5-di(2,4-dichlorophenyl)-2(5*H*)-furanone (**2h**) reduced the viability of *S. aureus* cells by 25.5% at 0.032 mg/mL (Table 3). However, higher concentrations of the butenolide did not improve the activity of this furanone. On the other hand, the best activity was obtained with **2d**, which, even if only a 0.7% death was observed at 0.032 mg/mL, it was able to eliminate 28.4% of the *S. aureus* viable cells at a higher concentration of 0.256 mg/mL.

For this reason, the dose used in the studies was increased to 0.512 mg/mL, observing that **2d** reduced cell viability by 47.5% (Figure 4). The kinetic studies revealed that at that concentration, *S. aureus* cells required longer periods of time to grow or proliferate. For example, the control without treatment required 6 h to grow; however, after treating with 0.512 mg/mL of **2d**, the bacterial cells required 10 h.

These results are of special interest since this molecule could be proposed for future studies to re-administer the drug before 10 h. Therefore, the dose of compound necessary to kill the microorganism could be reduced. In addition, the butenolides could be tested in

Table 3. Percentage of death at 0.032 mg/mL in the tested dimeric furanones (2) against *S. aureus*

Dimeric Furanones	Death % at 0.032 mg/mL
4-MeO (**2d**)	0.70
2-Naphthyl (**2f**)	0.60
4-Cl (**2g**)	17.00
2,4-Dicloro (**2h**)	25.53
4-Fluor (**2j**)	5.10
4-CN (**2l**)	0.00

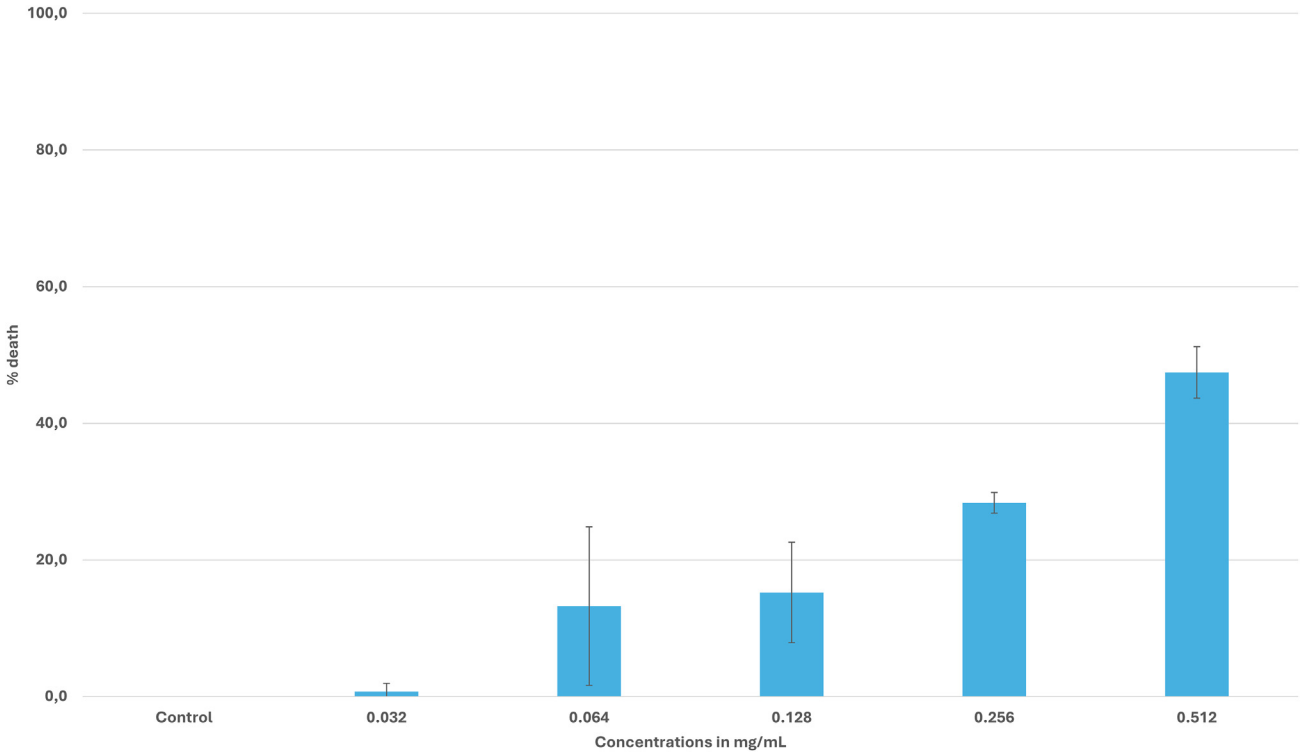

Figure 4. Percentage of death in *S. aureus* after treatment with 2d

combination with commercial compounds to increase their activity and reduce effective concentrations, which are cytotoxic and may increase drug resistance.

Conclusion

An undescribed, fast, and environmentally friendly electrochemical protocol for the room temperature synthesis of a variety of diarylated dimeric butenolides **2(a-l)** is now presented starting from their corresponding diarylated furans **1(a-l)**. This one-pot C-C-homocoupling reaction proceeds at Pt anode in aqueous acetonitrile media under constant current conditions. Mechanism proposals in the formation of **2** are discussed and supported by DFT theoretical calculations and furanoxy radical intermediate detection by EPR analysis and the fact that it was trapped by BHT or *p*-benzoquinone affording the corresponding adducts. The interesting influence of water, that conditions the appearance of the voltametric peak of **1**, allows, after the successive stages described here, to access bis-lactones **2** with good yield. Finally, the biocidal activity against *Staphylococcus aureus* of the obtained butenolides is now shown.

Limitations of the study

The very low solubility of the dimeric butenolides (**2**) in common organic solvents (and deuterated solvents) made it very difficult to perform in some cases well-resolved NMR spectra that, in the absence of X-ray analysis (that exceptionally was described[36] for **1b**) precluded a full and complete characterization of some of the obtained products. Furthermore, the formation of hydroxyl radicals from water under our experimental conditions has not been unambiguously proved.

RESOURCE AVAILABILITY

Lead contact

Further information and requests for resources should be directed to and will be fulfilled by the lead contact, Belen Batanero (belen.batanero@uah.es).

Materials availability

All strains used in this study can be ordered to Colección Española de Cultivos Tipo (CECT).

All other data supporting the findings of this study are available within the article and the supplemental information or can be obtained from the lead contact upon reasonable request.

Data and code availability

- All data reported in this paper is available within the paper or supplemental information on the web and will be shared by the lead contact upon request.
- This paper does not report original code.
- Any additional information required to reanalyze the data reported in this paper is available from the lead contact upon request.

ACKNOWLEDGMENTS

This work was supported by the University of Alcala project PIUAH23/CC-017 and Ministerio español de Ciencia e Innovación: projects PID2021-126877NA-I00 and PID2020-113274RA-I00/AEI/10.13039/501100011033.

Dedicated to the memory of Prof. Fructuoso Barba, on his 5th death anniversary.

AUTHOR CONTRIBUTIONS

Synthetic and chemical contributions: conceptualization: B.B.; methodology: N.S., E.P.-G., L.H., and S.E.-R.; formal analysis and investigation: B.B., N.S., E.P.-G., and L.H.; DFT theoretical calculations: M.T.Q.; writing original draft preparation: B.B.; review and editing: all authors; funding acquisition: B.B. and M.T.Q.; resources: all authors; supervision: B.B. and M.T.Q.

Microbiological contribution: conceptualization: J.L.C.-P., I.H.-B., and N.G.-C.; methodology: N.G.-C. and I.H.-B.; formal analysis and investigation: N.G.-C., J.L.C.-P., and I.H.-B.; data curation: N.G.-C. and I.H.-B.; writing original draft preparation: N.G.-C. and I.H.-B.; writing – review and editing: all authors; funding acquisition: J.L.C.-P. and I.H.-B.; resources: all authors; supervision: I.H.-B. and J.L.C.-P.

All authors have read and agreed to the published version of the manuscript.

DECLARATION OF INTERESTS

The authors declare no competing interest.

STAR★METHODS

Detailed methods are provided in the online version of this paper and include the following:

- KEY RESOURCES TABLE
- METHOD DETAILS
  - General information
  - Synthesis of 2,4-diarylfuranes 1
  - Synthesis of Furanones 2
  - Spectroscopic details of Furanones 2
  - Antibacterial activity of Butenolides 2

SUPPLEMENTAL INFORMATION

Supplemental information can be found online at https://doi.org/10.1016/j.isci.2024.110765.

Received: December 15, 2023
Revised: June 13, 2024
Accepted: August 14, 2024
Published: August 22, 2024

REFERENCES

1. Pandey, A.R., Singh, S.P., Joshi, P., Srivastav, K.S., Srivastava, S., Yadav, K., Chandra, R., Bisen, A.C., Agrawal, S., Sanap, S.N., et al. (2023). Design, synthesis and evaluation of novel pyrrole-hydroxybutenolide hybrids as promising antiplasmodial and anti-inflammatory agents. Eur. J. Med. Chem. *254*, 115340. https://doi.org/10.1016/j.ejmech.2023.115340.
2. Periche, P.G., Lin, J., Bhupathiraju, N.V.S.D.K., Kalidindi, T., Johnson, D.S., Pillarsetty, N., and Mootoo, D.R. (2023). Targeting Carbohydrate Mimetics of Tetrahydrofuran-Containing Acetogenins to Prostate Cancer. Molecules *28*, 2884. https://doi.org/10.3390/molecules28072884.
3. Wu, Y.M., Yang, X.Q., Chen, J.X., Wang, T., Li, T.R., Liao, F.R., Liu, R.T., Yang, Y.B., and Ding, Z.T. (2023). A new butenolide with antifungal activity from solid co-cultivation of *Irpex lacteus* and *Nigrospora oryzae*. Nat. Prod. Res. *37*, 2243–2247. https://doi.org/10.1080/14786419.2022.2037589.
4. Li, Y., Zhang, T., Ma, H., Xu, L., Zhang, Q., He, L., Jiang, J., Zhang, Z., Zhao, Z., and Wang, M. (2023). Design, Synthesis, and Antifungal/Antioomycete Activity of Thiohydantoin Analogues Containing Spirocyclic Butenolide. J. Agric. Food Chem. *71*, 6249–6267. https://doi.org/10.1021/acs.jafc.2c09144.
5. Fan, H., Wei, X., Si-Tu, M.X., Lei, Y.H., Zhou, F.G., and Zhang, C.X. (2022). γ-Aromatic Butenolides of Microbial Source - A Review of Their Structures, Biological Activities and Biosynthesis. Chem. Biodivers. *19*, e202200208. https://doi.org/10.1002/cbdv.202200208.
6. Hermens, J.G.H., Freese, T., Alachouzos, G., Lepage, M.L., Van Den Berg, K.J., Elders, N., and Feringa, B.L. (2022). A sustainable polymer and coating system based on renewable raw materials. Green Chem. *24*, 9772–9780. https://doi.org/10.1039/D2GC03657F.
7. Wang, X.J., and Hong, M. (2020). Lewis-Pair-Mediated Selective Dimerization and Polymerization of Lignocellulose-Based β-Angelica Lactone into Biofuel and Acrylic Bioplastic. Angew Chem. Int. Ed. Engl. *59*, 2664–2668. https://doi.org/10.1002/anie.201913136.
8. Hermens, J.G.H., Freese, T., van den Berg, K.J., van Gemert, R., and Feringa, B.L. (2020). A coating from nature. Sci. Adv. *6*, eabe0026. https://doi.org/10.1126/sciadv.abe0026.
9. Lepage, M.L., Alachouzos, G., Hermens, J.G.H., Elders, N., van den Berg, K.J., and Feringa, B.L. (2023). Electron-Poor Butenolides: The Missing Link between Acrylates and Maleic Anhydride in Radical Polymerization. J. Am. Chem. Soc. *145*, 17211–17219. https://doi.org/10.1021/jacs.3c04314.

10. Zhou, Y., Guo, S., Huang, Q., Lang, Q., Chen, G.-Q., and Zhang, X. (2023). Facile access to chiral γ-butyrolactones via rhodium-catalysed asymmetric hydrogenation of γ-butenolides and γ-hydroxybutenolides. Chem. Sci. *14*, 4888–4892. https://doi.org/10.1039/d3sc00491k.
11. Recnik, L.M., Thatcher, R.J., Mallah, S., Butts, C.P., Collingridge, G.L., Molnar, E., Jane, D.E., and Willis, C.L. (2021). Synthesis and pharmacological characterisation of arctigenin analogues as antagonists of AMPA and kainate receptors. Org. Biomol. Chem. *19*, 9154–9162. https://doi.org/10.1039/d1ob01653a.
12. Tadiparthi, K., and Venkatesh, S. (2022). Synthetic approaches toward butenolide-containing natural products. J. Heterocycl. Chem. *59*, 1285–1307. https://doi.org/10.1002/jhet.4480.
13. Yanai, H., Marquez, M.R., Cembellin, S., Martinez del Campo, T., and Almendros, P. (2023). Indium-promoted butenolide synthesis through consecutive C–C and C–O bond formations in aqueous tetrahydrofuran enabled by radicals. Org. Chem. Front. *10*, 1773. https://doi.org/10.1039/D3QO00133D.
14. Wu, X.-F., Sundararaju, B., Anbarasan, P., Neumann, H., Dixneuf, P.H., and Beller, M. (2011). A general cyclocarbonylation of aryl bromides and triflates with acetylenes: palladium-catalyzed synthesis of 3-alkylidenefuran-2-ones. Chem. Eur J. *17*, 8014–8017. https://doi.org/10.1002/chem.201101083.
15. Schacht, M., Boehlich, G.J., de Vries, J., Bertram, S., Gabriel, G., Zimmermann, P., Heisig, P., and Schützenmeister, N. (2017). Protecting-Group-Free Total Syntheses of Rubrolide R and S. Eur. J. Org. Chem. *2017*, 1745–1748. https://doi.org/10.1002/ejoc.201700158.
16. Finencio, B., Santos, F.A., and Laurentiz, R.S. (2023). Synthesis of β-Arylbutenolides Mediated by $BF_3{\cdot}OMe_2$. Synlett *34*, 77–80. https://doi.org/10.1055/s-0042-1753061.
17. Rossi, R., Bellina, F., and Raugei, E. (2000). Selective synthesis of unsymmetrical 3,4-disubstituted and 4-substituted 2(5H)-furanones. Synlett *2000*, 1749–1752. https://doi.org/10.1055/s-2000-8674.
18. Volger, H.C., Brackman, W., and Lemmers, J.W.F.M. (1965). The copper-catalysed oxidation of unsaturated carbonyl compounds Part III†: Oxidation of α,β- and β,γ-unsaturated aldehydes and ketones by oxygen in the presence of cupric complexes. Recl. Trav. Chim. Pays. Bas. *84*, 1203–1229. https://doi.org/10.1002/recl.19650840913.
19. Gopidas, K.R., Cyr, D.R., Das, P.K., and George, M.V. (1987). Photochemical and thermal transformations of 3-benzyl-2(3*H*)-furanones and related substrates. J. Org. Chem. *52*, 5505–5511. https://doi.org/10.1021/jo00234a002.
20. Bhattacharyya, K., Das, P.K., Fessenden, R.W., George, M.V., Gopidas, K.R., Hiratsuka, H., Hug, G.L., Rajadurai, S., and Samanta, A. (1989). Fluorescence studies of furanoxy radicals: intramolecular and intermolecular processes. J. Am. Chem. Soc. *111*, 3542–3548. https://doi.org/10.1021/ja00192a009.
21. Katsumura, S., Hori, K., Fujiwara, S., and Isoe, S. (1985). Regiospecific synthesis of γ-hydroxybutenolide. Photosensitized oxygenation of substituted 2-trimethylsilylfuran. Tetrahedron Lett. *26*, 4625–4628. https://doi.org/10.1016/S0040-4039(00)98769-0.
22. Patil, S.N., and Liu, F. (2007). Base-assisted regio- and diastereoselective conversion of functionalized furans to butenolides using singlet oxygen. Org. Lett. *9*, 195–198.
23. Yan, Z., Wei, W., Xun, H., and Anguo, S. (2012). Rose Bengal Immobilized on Wool as an Efficiently "Green" Sensitizer for Photooxygenation Reactions. Chem. Lett. *41*, 1500–1502. https://doi.org/10.1246/cl.2012.1500.
24. Bao, J., Tian, H., Yang, P., Deng, J., and Gui, J. (2020). Modular Synthesis of Functionalized Butenolides by Oxidative Furan Fragmentation. Eur. J. Org. Chem. *2020*, 339–347. https://doi.org/10.1002/ejoc.201901613.
25. Zvarych, V., Nakonechna, A., Marchenko, M., Khudyi, O., Lubenets, V., Khuda, L., Kushniryk, O., and Novikov, V. (2019). Hydrogen Peroxide Oxygenation of Furan-2-carbaldehyde via an Easy, Green Method. J. Agric. Food Chem. *67*, 3114–3117. https://doi.org/10.1021/acs.jafc.8b06284.
26. Torii, S., Tanaka, H., Ogo, H., and Yamasita, S. (1971). Anodic Reaction of 5-Alkyl-2-furoic Acids in Protic Solvents. Bull. Chem. Soc. Jpn. *44*, 1079–1084. https://doi.org/10.1246/bcsj.44.1079.
27. Cembellin, S., and Batanero, B. (2021). Organic Electrosynthesis Towards Sustainability: Fundamentals and Greener Methodologies. Chem. Rec. *21*, 2453–2471. https://doi.org/10.1002/tcr.202100128.
28. Eberson, L. (1967). Mechanism of the Kolbe electrosynthesis. Electrochim. Acta *12*, 1473–1478. https://doi.org/10.1016/0013-4686(67)80061-6.Vijh, A.K., and Conway, B.E. (1967). Electrode Kinetic Aspects of the Kolbe Reaction. Chem. Rev. *67*, 623–664. https://doi.org/10.1021/cr60250a003.
29. Schäfer, H.-J. (2001). Organic Electrochemistry. In Electrolytic Oxidative Coupling, 4th edition, H. Lund and O. Hammerich, eds. (CRC Press), pp. 883–967. CAN: 134:199740. https://doi.org/10.1201/9781420029659.
30. Weinberg, N.L., and Weinberg, H.R. (1968). Electrochemical oxidation of organic compounds. Chem. Rev. *68*, 449–523. https://doi.org/10.1021/cr60254a003.
31. Adams, R.N. (1969). Anodic oxidation pathways of aromatic hydrocarbons and amines. Acc. Chem. Res. *2*, 175–180. https://doi.org/10.1021/ar50018a003.
32. Hioki, Y., Costantini, M., Griffin, J., Harper, K.C., Merini, M.P., Nissl, B., Kawamata, Y., and Baran, P.S. (2023). Overcoming the limitations of Kolbe coupling with waveform-controlled electrosynthesis. Science *380*, 81–87. https://doi.org/10.1126/science.adf4762.
33. Hansen, B.H., and Dryhurst, G. (1971). Electrochemical oxidation of theophylline at the pyrolytic graphite electrode. J. Electroanal. Chem. *32*, 405–414. https://doi.org/10.1016/S0022-0728(71)80143-2.
34. Rosa, L.F., Röhring, K., and Harnisch, F. (2024). Electrolysis of medium chain carboxylic acids to aviation fuel at technical scale. Fuel *356*, 129590. https://doi.org/10.1016/j.fuel.2023.129590.
35. Zeng, C., Wang, B., Zhang, H., Sun, M., Huang, L., Gu, Y., Qiu, Z., Müllen, K., Gu, C., and Ma, Y. (2021). Electrochemical Synthesis, Deposition, and Doping of Polycyclic Aromatic Hydrocarbon Films. J. Am. Chem. Soc. *143*, 2682–2687. https://doi.org/10.1021/jacs.0c13298.
36. Quintanilla, M.G., Perez, I., Francisco de, B., Martin, A., Salardon, N., Fuente de la, J.L., and Batanero, B. (2021). New insights into the phenacyl bromide electroreduction: Unambiguously characterized 5,5′-bis(3,5-diaryl-2(5H)-furanone). Anodic oxidation of 2,4-diphenylfuran. J. Electroanal. Chem. *892*, 115265. https://doi.org/10.1016/j.jelechem.2021.115265.
37. Salinas, G., Arnaboldi, S., Garrigue, P., and Kuhn, A. (2023). Controlled Patterning of Complex Resistance Gradients in Conducting Polymers with Bipolar Electrochemistry. Adv. Mater. Interfac. *10*, 2202367. https://doi.org/10.1002/admi.202202367.
38. Figa, V., Luc, J., Baitoul, M., and Sahraoui, B. (2008). NLO properties of polythiophenes galvanostatically electrodeposited on ITO glasses. J. Optoelectron. Adv. Mater. *10*, 2123–2128.
39. Sheberla, D., Patra, S., Wijsboom, Y.H., Sharma, S., Sheynin, Y., Haj-Yahia, A.-E., Barak, A.H., Gidron, O., and Bendikov, M. (2015). Conducting polyfurans by electropolymerization of oligofurans. Chem. Sci. *6*, 360–371. https://doi.org/10.1039/C4SC02664K.
40. Lin, C.L., Wu, Y.-L., Chen, C.L., Chou, C.M., and Luh, T.-Y. (2007). Sequential Electrochemical Oxidation of Alternating Benzene-Furan Oligomers. J. Org. Chem. *72*, 8531–8534. https://doi.org/10.1021/jo070999+.
41. Schäfer, H.-J. (1990). Recent contributions of Kolbe electrolysis to organic synthesis. Top. Curr. Chem. *152*, 91–151.
42. Corey, E.J., Bauld, N.L., La Londe, R.T., Casanova, J., Jr., and Kaiser, E.T. (1960). Generation of cationic carbon by anodic oxidation of carboxylic acids. J. Am. Chem. Soc. *82*, 2645–2646. https://doi.org/10.1021/ja01495a066.
43. Solaja, B.A., Milic, D.R., and Gasic, M.J. (1996). A novel m-CPBA oxidation: p-quinols and epoxyquinols from phenols. Tetrahedron Lett. *37*, 3765–3768. https://doi.org/10.1016/0040-4039(96)00677-6.
44. Law, H.D., and Perkin, F.M. (1905). Electrolytic oxidation of hydrocarbons of the benzene series. Part II., ethyl benzene, cumene and cymene. Trans. Faraday Soc. *1*, 251–261. https://doi.org/10.1039/TF9050100251.
45. Ross, S.D., Finkelstein, M., and Uebel, J.J. (1969). Chemical and electrochemical oxidation of 2,5-dimethylfuran to 2,5-dimethyl-2,5-dimethoxydihydrofuran. J. Org. Chem. *34*, 1018–1020. https://doi.org/10.1021/jo01256a055.
46. Baizer, M.M. (1973). Organic Electrochemistry: An Introduction and a Guide (Dekker Inc.), p. 1072. CAN: 79:152274.
47. Andreades, S., and Zahnow, E.W. (1969). Anodic cyanations of aromatic compounds. J. Am. Chem. Soc. *91*, 4181–4190. https://doi.org/10.1021/ja01043a028.
48. Nørskov, J.K., Rossmeisl, J., Logadottir, A., Lindqvist, L., Kitchin, J.R., Bligaard, T., and Jónsson, H. (2004). Origin of the Overpotential for Oxygen Reduction at a Fuel-Cell Cathode. J. Phys. Chem. B *108*, 17886–17892. https://doi.org/10.1021/jp047349j.
49. Gaussian 16; Revision B.01, Frisch, M.J., Trucks, G.W., Schlegel, H.B., Scuseria, G.E., Robb, M.A., Cheeseman, J.R., Scalmani, G., Barone, V., et al. (2016) (Gaussian, Inc.).

50. Barba, F., Velasco, M.D., and Guirado, A. (1981). Electrochemical Synthesis of 2,4-Diarylfurans. Synthesis *1981*, 625–626. https://doi.org/10.1055/s-1981-29548.

51. Barba, F., Velasco, M.D., and Guirado, A. (1983). Cathodic reduction of phenacyl bromide. Electrochim. Acta *28*, 259–260. https://doi.org/10.1016/0013-4686(83)85118-4.

52. Yates, P., and Mayfield, R. (1977). A detailed assignment of the O–H stretching bands of ice I. Can. J. Chem. *55*, 3429–3441. https://doi.org/10.1139/v77-481.

53. Sato, T., Tamura, K., Maruyama, K., and Ogawa, O. (1973). The photooxidation of dypnone and p-substituted dypnones in the presence of metallic compounds. Tetrahedron Lett. *14*, 4221–4224. https://doi.org/10.1016/S0040-4039(01)87154-9.

54. Xu, P., Xie, J., Wang, D.-S., and Zhang, X.P. (2023). Metalloradical approach for concurrent control in intermolecular radical allylic C-H amination. Nat. Chem. *15*, 498–507. https://doi.org/10.1038/s41557-022-01119-4.

STAR★METHODS

KEY RESOURCES TABLE

REAGENT or RESOURCE	SOURCE	IDENTIFIER
Bacterial and virus strains		
Staphylococcus aureus	Colección de Cultivos Tipo (CECT)	CECT 240
Chemicals, peptides, and recombinant proteins		
2-Bromoacetophenone	Sigma-Aldrich	115835
2-Bromo-4′-methylacetophenone	Sigma-Aldrich	159530
4′-Propylacetophenone	Alfa Aesar	11354474
2-Bromo-4′-methoxyacetophenone	Sigma-Aldrich	115665
2-Bromo-4′-ethoxyacetophenone	Cymitquimica	AN-AG00DIG2
2-Bromo-2′-acetonaphthone	Sigma-Aldrich	105120
2-Bromo-4′-chloroacetophenone	Sigma-Aldrich	101273
2,2′,4′-Trichloroacetophenone	Sigma-Aldrich	159255
2,4′-Dibromoacetophenone	Sigma-Aldrich	D38308
2-Bromo-4′-fluoracetophenone	Sigma-Aldrich	389390
2-Bromo-4′-(methylsulfonyl)acetophenone	Fisher Scientific	B257325G
2-Bromo-4′-cyanoacetophenone	Sigma-Aldrich	539392
TEMPO, free radical	Alfa Aesar	A12733
BHT (2,6-di-tert-butyl-4-methyl-phenol)	Merck	B1215000
Benzoquinone	Sigma-Aldrich	B-10358
Lithium perchlorate (dry)	Sigma-Aldrich	62580F
Sodium perchlorate monohydrate	Scharlab S. L.	SO05350500
Bu_4NClO_4	Acros Organics	420141000
Et_4NBr	Sigma-Aldrich	14,002-3
Acetonitrile	Scharlab S. L.	AC03292500
MeOH	Scharlab S. L.	ME03151000
DMF	Alfa Aesar	A13547
$CDCl_3$	Scharlab S. L.	CL12130500
DMSO-d_6	Euriso-top	D010ES
CD_3-OD	Euriso-top	D024ES
Acetone-d_6	Euriso-top	D009ES
Mueller Hinton Broth medium	Scharlab S. L.	02-136-500
DMSO	Thermo Scientific	85190
PCA	Scharlab S. L.	01-161-500
Software and algorithms		
ChemDraw Professional 12.0	PerkinElmer	https://www.perkinelmer.com/category/chemdraw
Gaussian16	Frish et al.[49]	https://gaussian.com
Other		
Voltammetry-Potentiostat	Radiometer Analytical	POL150-TraceMaster
Current supplier	PROMAX	Model FAC-662B
Potentiostat	Amel	Model 552
electronic Coulombimeter integrator	Amel	Model 721

(*Continued on next page*)

Continued

REAGENT or RESOURCE	SOURCE	IDENTIFIER
IR spectrophotometer	Perkin-Elmer FT-IR	Frontier
MS spectrometer	THERMOFISHER	ITQ-900
NMR spectrometry	Varian/Brucker	Unity 300/500 MHz
Electron paramagnetic resonance (EPR)	Brucker spectrometer	Model Magnettech ESR5000

METHOD DETAILS

General information

The electrolyses were carried out using a constant current supplier (galvanostat) PROMAX Model FAC-662B or a constant potential Amel potentiostat, Model 552, connected with an electronic coulombimeter integrator Amel, Model 721. Cyclic voltammetry was recorded on a VoltaLab/TraceMaster Radiometer Analytical Potentiostat, Model PGZ100/POL150. Electron paramagnetic resonance (EPR) was performed in an Brucker spectrometer Model Magnettech ESR5000. IR spectra of the products were recorded as dispersions in KBr on a Perkin-Elmer FT-IR Frontier spectrometer. Mass spectra (EI, ionizing voltage 70 eV or CI chemical ionization with methane) were determined using a THERMOFISHER ITQ-900 DIP or GC-MS mass-selective detector. ^{1}H, ^{13}C NMR, correlation COSY, HSQC, HMBC and other resonance spectra were recorded in $CDCl_3$, CD_3OD, Pyridine-d_5, THF-d_8 or DMSO-d_6 on a Varian Unity 300 (300 MHz & 75.4 MHz for ^{1}H and ^{13}C respectively) or a Brucker 500 MHz spectrometers, with tetramethylsilane (TMS) as the internal standard. The chemical shifts are given in ppm. All melting points were measured on a Reichert Thermovar microhot stage apparatus and are uncorrected. All starting materials were obtained from commercial sources and used without purification.

Synthesis of 2,4-diarylfuranes 1

Previous publications from this laboratory have dealt with phenacyl bromides electroreduction[50,51] to prepare 2,4-diarylfuranes **1(a-l)** as the starting material. The physical and spectroscopical properties of the undescribed starting 2,4-diarylfurans are summarized in the Supporting Information file, together with their corresponding spectra.

Synthesis of Furanones 2

A solution of 2,4-diarylfuran (**1**) (0.25 mmol, or 0.5 mmol) in 40 mL of dry acetonitrile/$LiClO_4$, acetonitrile-H_2O (20%) (40:10), acetonitrile-H_2O (20:5)/(0.1 M) $NaClO_4$ or DMF-H_2O (20:5)/(0.1 M) $NaClO_4$ was electrolyzed under an argon atmosphere to exclude air, at a platinum sheet (8 cm^2) as the working electrode and a smaller platinum sheet (4 cm^2) as auxiliary electrode under constant current (10/30/50 mA) or constant potential (+ 1.3 V *vs* Ag/Ag^+) conditions. Anodic peak potential (E_{pa}) was previously determined by cyclic voltammetry (Figures 2 and S1). A slight excess of current (4 Faradays had passed per mol of starting material) was required to complete the reaction. The main electrolysis experiments were performed at room temperature (25°C), or at 15°C in a concentric beaker-type electrochemical reactor with two compartments separated by a porous (D4) glass frit diaphragm and equipped with a magnetic stirrer. During electrolysis, the anodic compartment acquires some white-yellow colour and increasing turbidity as dimeric butenolide (**2**) is being formed, due to its insolubility in the reaction medium.

Once the reaction was finished, the white solid from the anodic solution was filtered, washed with cold acetonitrile-distilled water and dried in vacuum. This solid was purified by column chromatography (when needed) in silica gel 60 (35-70 mesh) using a (15 x 2 cm) column, and CH_2Cl_2 as eluent and characterized as 5,5′-bis(3,5-diaryl-2(5*H*)-furanone) **2(a-l)**, being the main product of the reaction. Further evaporation of the acetonitrile filtrate solution provided a green-blue residue that was three times extracted with chloroform (to separate the electrolyte). The organic layers were joined and dried over Na_2SO_4 and then concentrated by reduced pressure. The final crude, resulting solid or oil, was analysed by TLC and chromatographed on a GC-MS (HP-5 crosslinked 5% PhMe silicone 30 m-0.25 mm-0.25µm chromatographic column) instrument. In some cases, the secondary product **3a** was separated by chromatography, in silica gel 60 (35-70 mesh) using a (25 x 2 cm) column, and $CHCl_3$: Hex (2:1) as eluent. Dimeric butenolides **2(a-l)** were isolated as a mixture of *meso* (*RS*) and diastereomeric (*RR/SS*) forms (in ratio 1:3 when Ar = Ph, however this ratio changes in other butenolides). Many of these bis-lactones proved to be very insoluble white solids, difficult to be dissolved in usual organic solvents. The physical and spectroscopical properties of the undescribed starting 2,4-diarylfurans are summarized in the Supporting Information file (together with spectra of **1** and **2**). The physical and spectroscopical properties of the undescribed dimeric butenolides is as follows:

Spectroscopic details of Furanones 2

Spectra of furanones **2** are available in the Supporting Information file. The physical and spectroscopical properties of the undescribed dimeric butenolides is as follows:

5,5′-Bis(3,5-diphenyl-2(5H)-furanone) (2a)

Mp 289-291ºC [Lit.[19] 285-288ºC].

5-Hydroxy-3,5-diphenyl-2(5H)-furanone (3a) (in equilibrium with *cis*-β-benzoylphenylacrylic acid)

Mp 122-124ºC [Lit.[52] 122-123ºC]. IR (KBr) ν_{max} = 3414, 3062, 2921, 1760, 1692, 1600, 1492, 1450, 1176, 969, 757, 697 cm^{-1}. ^{1}H NMR (300 MHz, $CDCl_3$) δ: 4.95 (bs, 1H), 7.39-7.44 (m, 7H), 7.63 (bs, 2H), 7.80-7.84 (m, 2H). ^{13}C NMR (75.4 MHz, $CDCl_3$) δ: 103.7, 125.6, 127.5, 128.7, 128.9, 130.0, 133.7, 137.3, 146.1, 171.2, 187.5. MS *m/z* (relative intensity) EI: 252 (M^+, 37), 235 (4), 224 (82), 207 (58), 179 (100), 178 (64), 165 (14), 152 (10), 147 (12), 130 (10), 119 (11), 105 (15), 103 (13), 102 (20), 91 (11), 77 (44).

5,5′-Bis(3,5-di(4-methylphenyl)-2(5H)-furanone) (2b)

meso-X-ray diffraction analysis.[36] Mp 261-262ºC [Lit.[19] 258-260ºC]. IR (KBr) ν_{max}= 3085, 3033, 2917, 1761, 1615, 1513, 1261, 1153, 1089, 1002, 969, 822 cm^{-1}. ^{1}H NMR (500 MHz, $CDCl_3$) δ: 2.23 (s, 6Hd), 2.29 (s, 6Hm), 2.30 (s, 6Hd), 2.32 (s, 6Hm), 7.04 (d, *J*= 7.8 Hz, 4Hm), 7.10 (d, *J*= 7.8 Hz, 8Hd), 7.17-7.19 (m, 8Hm), 7.37 (d, *J*= 7.8 Hz, 4Hd), 7.42 (d, *J*= 7.8 Hz, 4Hd), 7.62 (d, *J*= 7.8 Hz, 4Hm), 7.76 (s, 2Hm), 7.87 (s, 2Hd). ^{13}C NMR (125 MHz, $CDCl_3$) δ: 21.0, 21.1, 21.3, 21.4, 89.5, 89.9, 124.0, 125.9, 126.0, 126.9, 127.0, 127.1, 128.7, 129.0, 129.2, 129.3, 130.9, 132.1, 132.7, 132.8, 138.7, 138.9, 139.6, 139.9, 145.7, 146.3, 169.6, 169.8. MS *m/z* (relative intensity) EI: 526 (M^+, 2), 263 (1/2 M^+, 100), 234 (7), 190 (5), 119 (95), 115 (11), 91 (28).

3,5-Di(4-methylphenyl)furan-2(5H)-one

GC-MS *m/z* (relative intensity) EI: 264 (M^+, 100), 236 (10), 207 (29), 192 (13), 145 (33), 119 (40), 91 (21).

5,5′-Bis(3,5-di(4-propylphenyl)-2(5H)-furanone) (2c)

Mp 189-190ºC. IR (KBr) ν_{max} = 3088, 3036, 2928, 1754, 1609, 1509, 1157, 1094, 997, 971 cm^{-1}. ^{1}H NMR (500 MHz, $CDCl_3$) δ: 0.75-0.95 (m, 12Hm+12Hd), 1.50-1.62 (m, 8Hm+8Hd), 2.49-2.58 (m, 8Hm+8Hd), 7.05 (d, *J*= 8.4 Hz, 4Hm), 7.10-7.14 (m, 8Hd), 7.17-7.19 (m, 8Hm,), 7.37 (d, *J*= 8.4 Hz, 4Hd), 7.47 (d, *J*= 8.4 Hz, 4Hd), 7.67 (d, *J*= 8.4 Hz, 4Hm), 7.83 (s, 2Hm), 7.88 (s, 2Hd). ^{13}C NMR (125 MHz, $CDCl_3$) δ: 13.4, 13.5, 13.7, 24.2, 24.3, 37.4, 37.5, 37.8, 89.6, 90.0, 126.2, 126.3, 126.8, 126.9, 127.2, 128.1, 128.4, 128.6, 128.8, 131.1, 132.4, 132.8, 133.0, 143.3, 143.6, 144.3, 144.7, 145.5, 146.5, 169.7, 169.9. MS *m/z* (relative intensity) EI: 638 (M^+, 0.5), 319 (1/2 M^+, 94), 290(100), 261(6), 173(4), 147(60), 118(7), 91(17).

5-Hydroxy-3,5-di(4-propylphenyl)-2(5H)-furanone (3c)

yellow oil. IR (KBr) ν_{max} = 3380, 2953, 2930, 1762, 1693, 1651, 1604, 1417, 1181, 1118, 945 cm^{-1}. ^{1}H NMR (300 MHz, $CDCl_3$) δ: 0.95 (t, J= 7.1 Hz, 6H), 1.64 (m, 4H), 2.60 (t, J= 7.4 Hz, 4H), 4.75 (bs, 1H), 7.10-7.22 (m, 4H), 7.40 (s, 1H), 7.49 (d, J= 8.0 Hz, 2H), 7.75 (d, J= 8.0 Hz, 2H). ^{13}C NMR (75.4 MHz, $CDCl_3$) δ: 13.7, 24.3, 37.7, 103.6, 125.4, 126.1, 127.0, 127.5, 128.6, 128.8, 128.9, 129.4, 131.2, 134.8, 145.3, 170.0. MS *m/z* (relative intensity) EI: 336 (M^+, 27), 308 (92), 293 (100), 279 (14), 263 (32), 249 (40), 247(36), 221 (22), 179 (28), 133 (10), 91 (17).

3,5-Di(4-propylphenyl)furan-2(5H)-one

GC-MS *m/z* (relative intensity) EI: 320 (M^+, 100), 264 (10), 263 (34), 249 (12), 173 (41), 147 (72), 115 (8), 91 (13).

5,5′-Bis(3,5-di(4-methoxyphenyl)-2(5H)-furanone) (**2d**)

Mp 229-231ºC. [Lit.[19] 230-233ºC]. IR (KBr) ν_{max} = 3441, 3091, 3010, 2956, 2837, 1756, 1608, 1512, 1460, 1301, 1263, 1251, 1158, 1087, 1028, 833 cm^{-1}.^{1}H NMR (500 MHz, DMSO-d_6) δ: 3.73 (s, 3Hm), 3.76 (s, 3Hm), 3.82 (s, 6Hd), 3.83 (s, 6Hd), 3.84 (s, 3Hm), 3.87 (s, 3Hm), 6.87 (d, *J*= 8.0 Hz, 8H), 6.94 (d, *J*= 8.2 Hz, 4H), 6.97 (d, *J*= 8.2 Hz, 4H), 7.32 (d, *J*= 8.0 Hz, 4H), 7.44 (d, *J*= 7.8 Hz, 4H), 7.68-7.71 (m, 8H), 8.73 (s, 2Hm), 8.75 (s, 2Hd). MS *m/z* (relative intensity) QI: 591 (M^++1, 0.7), 296 (1/2 M^++1, 100), 295 (1/2 M^+, 86), 279(14), 251 (11), 189 (10), 161 (7), 135 (15).

3,5-Di(4-methoxyphenyl)furan-2(5H)-one

GC-MS *m/z* (relative intensity) EI: 296 (M^+, 100), 268 (12), 239 (22), 224 (8), 161 (43), 135 (40), 77 (7).

1,3-Bis(4-methoxyphenyl)-2-propen-1-one

(obtained after decarboxylation of 2,4-bis(4-methoxyphenyl)-4-oxobut-2-enoic acid, obtained by the hydrolysis of **3d**). GC-MS *m/z* (relative intensity) EI: 268 (M^+, 100), 253 (45), 237 (20), 225 (32), 160 (7), 108 (6).

5,5′-Bis(3,5-di(4-ethoxyphenyl)-2(5H)-furanone) (**2e**)

Mp 173-174ºC. IR (KBr) ν_{max} = 3425, 3096, 2981, 2931, 1756, 1680, 1612, 1512, 1468, 1387, 1302, 1255, 1181, 1157, 1118, 1084, 1044, 968, 837 cm^{-1}. ^{1}H NMR (500 MHz, DMSO-d_6) δ: 1.22-1.34 (m, 12Hm+12Hd), 3.92-4.04 (m, 8Hm+8Hd), 6.74 (d, *J*= 8.6 Hz, 2Hm), 6.84 (d, *J*= 8.6 Hz, 6Hd), 6.92 (d, *J*= 8.5 Hz, 4Hm), 6.96 (d, *J*= 8.5 Hz, 4Hm), 7.05 (d, *J*= 8.6 Hz, 2Hm), 7.30 (d, *J*= 8.6 Hz, 2Hd), 7.41 (d, *J*= 8.6 Hz, 4Hd), 7.67 (d, *J*= 8.6 Hz, 2Hm+ 2Hd), 7.70 (d, *J*= 8.6 Hz, 2Hd), 7.75 (d, *J*= 8.6 Hz, 2Hm), 8.70 (s, 2Hm), 8.71 (s, 2Hd).^{13}C NMR (75.4 MHz, DMSO-d_6) δ: 14.8, 14.9, 63.5, 63.6, 89.9, 90.4, 114.0, 114.1, 114.9, 115.0, 121.5, 121.6, 126.5, 126.6, 128.8, 129.3, 130.9, 131.0, 131.1, 131.7, 147.1, 147.8, 158.9, 159.8, 159.9, 162.7, 169.9. MS *m/z* (relative intensity) EI: 646 (M^+, 0.1), 323 (1/2 M^+, 100), 294 (48), 266 (30), 238 (7), 210 (14), 175 (16), 149 (73), 121 (40), 65 (5).

5,5′–Bis(3,5-di(naphthalen-2-yl)-2(5H)-furanone (2f)

Mp 310-311°C. Highly insoluble solid. IR (KBr) ν_{max} = 3435, 3088, 3059, 1754, 1636, 1599, 1212, 1149, 1086, 984, 821, 745 cm^{-1}. ^{1}H NMR (500 MHz, Pyridine-d_5) δ: 7.02 (s, 2Hm), 7.35– 7.46 (m, 10Hm), 7.70– 7.77 (m, 6Hd), 7.80-7.85 (m, 4Hm), 7.87-7.93 (m, 5Hd), 8.09 (d, *J*= 8.0 Hz, 3Hd), 8.31 (s, 2Hm), 8.56 (s, 2Hm), 8.60 (s, 2Hm), 8.91 (d, *J*= 8.0 Hz, 2Hd), 9.25 (s, 2Hm), 9.37 (s, 2Hd). ^{1}H NMR (500 MHz, $CDCl_3$) δ: 7.40-7.60 (m, 6Hd+14Hm), 7.63-7.94 (m, 20Hd+8Hm), 8.07 (s, 2Hm), 8.20 (s, 2Hm), 8.31 (bs, 2Hd), 8.62 (s, 2Hm), 8.69 (s, 2Hd). ^{13}C NMR (125 MHz, Pyridine-d_5) δ: 91.0, 124.8, 125.5, 126.9, 127.1, 127.5, 127.9, 128.0, 128.7, 128.9, 132.5, 133.2, 133.5, 134.0, 139.2, 149.1, 170.0. gHMBC (DMSO-d_6) correlation ^{13}C NMR δ: 90.6 ppm with ^{1}H NMR δ: 9.25 ppm.

3,5-Di(naphthalen-2-yl)furan-2(5H)-one

GC-MS *m/z* (relative intensity) EI: 336 (M^+, 100), 307 (10), 289 (14), 279 (23), 181 (25), 155 (70), 152 (24), 127 (28), 75 (3).

5,5′–Bis(3,5-di(4-chlorophenyl)-2(5H)-furanone (2g)

Mp 220–221°C. Highly insoluble solid. IR (KBr) ν_{max} = 3432, 3083, 1763, 1636, 1588, 1492, 1407, 1156, 1092, 970, 831, 769 cm^{-1}.^{1}H NMR (500 MHz, DMSO-d_6) δ: 7.40-7.57 (m, 12Hd+12Hm), 7.74 (d, *J*= 8.6 Hz, 4Hd), 7.80 (d, *J*= 8.6 Hz, 4Hm), 8.97 (s, 2Hm), 9.03 (s, 2Hd). gHMBC (DMSO-d_6) correlation ^{13}C NMR δ: 90 ppm with ^{1}H NMR δ: 8.97 and 9.03 ppm. MS *m/z* (relative intensity) EI: 575 (M^++2-35, 1), 305 (1/2 M^++4, 30), 304 (1/2 M^++2, 15), 303 (1/2 M^+, 42). MS *m/z* (relative intensity) QI: 608 (M^++2, 1), 606 (M^+, 3), 575 (M^++2-35, 100), 573 (M^+-35, 70), 542 (28), 540 (27), 434 (5), 436 (4). MS-ESI-High Resolution QTOF of 2g (m/z = 571: M+- Cl).

3,5-di(4-chlorophenyl)furan-2(5H)-one

GC-MS *m/z* (relative intensity) EI: 306 (M^++2, 30), 304 (M^+, 43), 271 (34), 269 (100), 243 (31), 241 (89), 178 (33), 139 (28), 111 (31), 75 (50).

5,5′–Bis(3,5-di(2,4-dichlorophenyl)-2(5H)-furanone (2h)

Mp 201-203°C. IR (KBr) ν_{max} = 3436, 3102, 1780, 1585, 1473, 1375, 1140, 1056, 967, 867, 811 cm^{-1}. ^{1}H NMR (500 MHz, DMSO-d_6) δ: 7.25-7.42 (m, 4Hd+6Hm), 7.43-7.49 (m, 4Hd+4Hm), 7.60-7.64 (m, 4Hd), 7.77 (d, *J*= 8.6 Hz, 2Hm), 9.01 (s, 2Hm, C*H*=), 9.07 (s, 2Hd, C*H*=). gHMBC (DMSO-d_6) correlation ^{13}C NMR δ: 91 ppm with ^{1}H NMR δ: 9.01 and 9.07 ppm. MS *m/z* (relative intensity) QI: 745 (M^++2+1, 1), 743 (M^++1, 1), 416 (4), 414 (0.5), 402 (14), 376 (50), 374 (100), 372 (64).

5,5′–Bis(3,5-di(4-bromophenyl)-2(5H)-furanone (2i)

Mp 239–241°C. [Lit.[53] 242-243ºC]. Highly insoluble solid. IR (KBr) ν_{max} = 3447, 3083, 1760, 1611, 1515, 1483, 1403, 1149, 1072, 1008, 928, 828, 807 cm^{-1}. ^{1}H NMR (500 MHz, DMSO-d_6) δ: 7.34-7.6 (m, 8Hm), 7.64-7.70 (m, 8Hm), 7.76 (d, J= 7.76 Hz, 8Hd), 7.94 (d, J= 7.9 Hz, 8Hd), 8.98 (s, 2Hm), 9.04 (s, 2Hd). ^{13}C NMR (75.4 MHz, DMSO-d_6) δ: 90.2, 123.8, 124.5, 128.4, 128.7, 130.0, 130.7, 131.0. 131.9, 132.2, 132.8, 132.9, 133.0, 133.9, 136.6, 150.4, 169.6. gHMBC (DMSO-d_6) correlation ^{13}C NMR δ: 90.2 ppm with ^{1}H NMR δ: 8.98 and 9.04 ppm. MS *m/z* (relative intensity) QI: 784 (M^++2, 4), 782 (M^+, 4), 755 (M^++2-*29*, 68), 753 (M^+-*29*, 100), 751 (62), 703 (7), 675 (68), 673 (68), 597 (16), 595 (27), 593 (16).

5,5′–Bis(3,5-di(4-fluorophenyl)-2(5H)-furanone (2j)

Mp 273–275°C. IR (KBr) ν_{max} = 3512, 3091, 2928, 1765, 1603, 1510, 1237, 1153, 968, 840 cm^{-1}. ^{1}H NMR (500 MHz, DMSO-d_6) δ: 7.15-7.35 (m, 16H), 7.40– 7.85 (m, 16H), 8.93 (s, 2Hm, C*H*=), 8.98 (s, 2Hd, C*H*=). ^{13}C NMR (75 MHz, DMSO-d_6) δ: 89.6, 115.4, 116.3, 122.2, 125.5, 129.8, 130.5, 131.2, 148.5, 149.4, 161.6, 169.3. gHMBC (DMSO-d_6) correlation ^{13}C NMR d: 89.6 and 89.9 ppm with ^{1}H NMR d: 8.98 and 8.93 ppm respectively. MS *m/z* (relative intensity) IQ: 543 (M^++1, 4), 372 (1/2 M^++1, 100), 371 (1/2 M^+, 50), 255 (44), 245 (13), 177 (8), 123 (7).

5,5′–Bis(3,5-di(4-(methylsulfonyl)phenyl)-2(5H)-furanone (2k)

Mp 289–291°C. IR (KBr) ν_{max} = 3437, 3088, 3002, 2923, 1770, 1669, 1598, 1408, 1307, 1151, 1089, 963, 771 cm^{-1}. ^{1}H NMR (300 MHz, DMSO-d_6) δ: 3.14 (s, 6H), 3.18 (s, 6H), 3.22 (s, 6H), 3.23 (s, 6H), 7.69 (d, J= 8.5 Hz, 4Hm), 7.82 (d, J= 8.5 Hz, 4Hd), 7.90–8.10 (m, 10Hm + 12Hd), 8.31 (s, 2Hm), 9.27 (s, 2Hm, C*H*=), 9.30 (s, 2Hd, C*H*=). ^{13}C NMR (75 MHz, DMSO-d_6) δ: 42.8 (SO_2*Me*), 88.8, 126.9, 127.4, 127.7, 130.5, 130.8, 132.5, 137.8, 141.1, 154.2, 167.5 (C=O).

5,5′-Bis(3,5-di(4-cyanophenyl)-2(5H)-furanone) (2l)

Mp 301-303ºC. IR (KBr) ν_{max} = 3441, 3094, 2231, 1769, 1608, 1503, 1415, 1154, 1087, 967, 844 cm^{-1}. ^{1}H NMR (500 MHz, DMSO-d_6) δ: 7.60-7.98 (m, 14Hm+14Hd), 8.14-8.17 (m, 1Hm+1Hd), 8.54 (s, 1Hm), 8.57 (s, 1Hd), 9.18 (s, 2Hm), 9.26 (s, 2Hd). gHMBC (DMSO-d_6) correlation ^{13}C NMR δ: 89.9 ppm with ^{1}H NMR δ: 9.18 and 9.26 ppm. MS *m/z* (relative intensity) IQ: 571 (M^++1, 0.5), 287 (100), 286 (40), 315 (18), 269 (16), 243 (12), 156 (4).

2-Bromo-3,5-diphenylfuran

Oil. [Lit.[54] Colorless oil]. ^{1}H NMR (300 MHz, $CDCl_3$) δ: 6.71 (s, 1H), 7.08-7.18 (m, 2H), 7.19-7.30 (m, 4H), 7.45-7.55 (m, 4H). ^{13}C NMR (75 MHz, $CDCl_3$) δ: 106.9, 118.1, 123.1, 125.9, 126.8, 127.1, 127.5, 128.2, 128.3, 129.3, 131.1, 155.1. MS *m/z* (relative intensity) EI: 300 (M^++2, 62), 292 (M^+, 62), 219 (23), 191 (100), 189 (41), 165(17), 95 (8).

3,5-Bis(4-chlorophenyl)-5-(2,5-dihydroxyphenyl)-2(5H)-furanone

MS *m/z* (relative intensity) EI: 416 (M^++4, 31), 414 (M^++2, 94), 412 (M^+, 100), 379 (15), 377 (30), 351 (4), 349 (8), 303 (14), 301 (27), 265 (10), 238 (9) , 208 (11), 202 (16), 139 (19).

3,5-Di-tert-butyl-4-hydroxybenzaldehyde

MS *m/z* (relative intensity) EI: 234 (M^+, 30), 219 (100), 203 (7), 191 (73), 175 (18), 91 (8).

5-(3,5-Di-tert-butyl-4-hydroxybenzyl)-3,5-diphenyl-2(5H)-furanone

MS *m/z* (relative intensity) EI: 454 (M^+, 40), 439 (12), 398 (38), 248 (100), 219 (27), 205 (14), 203 (21), 147 (4), 105 (9).

Antibacterial activity of Butenolides 2

Furanones have been proven to possess antibacterial activity against different microorganisms. Infectious diseases caused by pathogenic bacteria are a mayor health concern, mainly associated with bacterial resistance to commercial antimicrobials/antibiotics. Consequently, there is an urgent need to find new compounds effective against these resistant microorganisms. Now described electro-synthesized furanones (**2**) were studied to determine their *in vitro* antibacterial activity against *Staphylococcus aureus*, a gram-possitive bacteria.

More information about the compound-bacteria interaction was obtained from kinetic studies (see below). Among all the molecules tested, **2d** and **2h** showed activity reducing microbial viability. These studies are promising and encourage us to carry out complementary studies to improve the structural composition of these molecules in order to increase their effectiveness against pathogenic bacteria.

In vitro antibacterial activity Tests

The microorganism used in the assays was a strain of *Staphylococcus aureus* (CECT 240, Gram-positive) provided by the Colección de Cultivos Tipo (CECT), Spain.

The assay was based on the ISO 20776-1:2006 protocol. First, colonies were transferred and grown in Mueller Hinton Broth medium in agitation at 150 rpm and 37°C for 24 h. Then, bacteria were incubated with dimeric furanones **2**. The range of concentrations study was from 0.004 mg/mL to 0.512 mg/mL. All of them were diluted in DMSO. The final dilutions used in the *in vitro* assays only contained 1% DMSO. Assays were run on technical triplicates in sterile 96-well plates. Also, different controls were added such as inoculum without compound, compound without inoculum and culture medium without inoculum and compound. Each well contained 100 μL of compound, 100 μL of medium and 5 μL of inoculum (10^7 CFU/mL). The microplates were incubated for 24 h at 37°C. Absorbance was measured at 630 nm in an Ultra Microplate reader (BIO-TEK Instruments, model ELx808, Winooski, Vermont, United States), at 20 h. Finally, 5 μL of each well was deposited on a petri dish with PCA medium and incubated for 24 h to obtain the minimum bactericidal concentration (MBC) values.

Kinetic studies

The kinetic studies were performed by measuring absorbance every hour for 20 h. Microplates were incubated at 37°C. The absorbances were measured at 630 nm. Samples were performed in triplicate. The data at each hour were analyzed by comparing the values of the different concentration gradients with the value of the control at the corresponding time. For each compound concentration and incubation time, the percentage of cell viability was calculated.